Current-induced magnetization switching in a microscale ring-shaped magnetic tunnel junction

Hong-Xiang Wei,[1] Mark C. Hickey,[2] Graham I. R. Anderson,[2] Xiu-Feng Han,[1,*] and Christopher H. Marrows[2,†]
[1]State Key Laboratory of Magnetism, Institute of Physics, Chinese Academy of Sciences, Beijing 100080, People's Republic of China
[2]School of Physics and Astronomy, University of Leeds, Leeds LS2 9JT, United Kingdom

(Received 20 August 2007; published 2 April 2008)

A current-induced magnetization switching has been observed in a microscale ring-shaped magnetic tunnel junction having an alumina barrier, which showed a tunneling magnetoresistance ratio of 37% and a resistance-area product of 175 $\Omega\ \mu m^2$. Several metastable magnetization states were observed during field driven switching of this junction. Preparing the junction in one of these metastable states allowed a current-induced switching to take place at current densities 2 orders of magnitude lower than conventional switching values. Micromagnetic modeling indicates that the effect was solely due to Oersted field switching, which explains the markedly different forms of the current- and field-driven hysteresis loops.

DOI: 10.1103/PhysRevB.77.132401 PACS number(s): 75.60.Nt, 75.47.Np, 72.25.−b

Magnetic tunnel junctions (MTJs) are archetypal spintronic systems, which show large magnetoresistances due to spin-polarized tunneling. They find application as hard drive read heads and magnetic random access memory cells.[1] MTJs patterned into rings are particularly interesting due to the stability of flux-closed micromagnetic states, which are possible in that topology.[2] The inverse effect to magnetoresistance, i.e., the current-excited magnetization dynamics in magnetic multilayers,[3,4] has been the subject of much research in recent years due to the new physics that can be studied, such as current-induced magnetization switching[5] (CIMS) and microwave generation.[6] CIMS in MTJs[7–9] is of particular interest for devices because of the large cell resistance and high tunneling magnetoresistance (TMR) signals that can be achieved.[10]

Two different effects can be placed in the CIMS bracket. The current can directly deliver spin angular momentum to the local magnetization, resulting in spin-torque switching.[3,4] On the other hand, the current generates an Oersted field, which can also affect the magnetization in the conventional way through the Zeeman energy term. Spin-torque switching is usually most easily observed in nanoscale devices as, for instance, in a recent report concerning junctions with either MgO or alumina barriers,[10] where Oersted fields are small. Oersted field switching was observed in microscale junctions via the formation of vortex states.[11–13] For both of these methods, the critical current for switching is still high: A typical figure for the critical switching current density (J_C) required with an AlO_x barrier is on the order of 10^6 A cm^{-2}.[11]

Here, we report observations of CIMS at much lower current densities in microscale ring-shaped MTJs, when the switching is not between fully parallel (P) and antiparallel (AP) states, but between metastable states that have already been partially switched using an applied magnetic field. The partial states are formed due to the inhomogeneous shape anisotropy field from the ring structure. The partially magnetized states and their current-induced switching have been micromagnetically modeled in order to explain the observations. Previously, CIMS was observed in rectangular microscale junctions where the current density needed was similar to that of nanojunctions and full switching between the AP and P states did not occur.[11] Those junctions were rectangular in shape, whereas the ones studied here were rings.

The MTJ structures were deposited onto a Si/SiO_2 substrate using an ultrahigh vacuum (ULVAC) sputtering system with a base pressure of 1×10^{-7} Pa and comprised the layers Ta (5)/IrMn (10)/$Co_{75}Fe_{25}$ (2)/Ru (0.75)/$Co_{40}Fe_{40}B_{20}$ (3)/Al (0.6)+O/$Co_{40}Fe_{40}B_{20}$ (2.5)/Ta (3)/Ru (5) (layer thicknesses in nanometers). The barrier was formed by depositing a thin Al layer, followed by exposure to an oxygen plasma to produce a disordered AlO_x barrier. The bottom CoFeB layer is pinned via an artificial antiferromagnetic multilayer, while the top CoFeB is free to switch between the P and AP states. The device we shall discuss here was a microscale MTJ ring, with an outer radius of 8 μm and an inner radius of 4 μm, and was patterned using standard UV lithography combined with ion milling so that both the free and pinned magnetic layers were ring shaped. All transport measurements were performed at room temperature using a conventional four-point probe setup. A positive conventional current corresponds to electrons flowing from the free layer to the pinned layer.

The active junction area of the ring was 150 μm^2, and the tunnel resistances when the magnetization of the free layer and pinned layer were aligned parallel (R_P) and antiparallel (R_{AP}) were 1.16 and 1.59 Ω, respectively, as shown in Fig. 1. The tunnel resistance was quite small due to the very thin barrier; subsequently, the resistance-area product was also quite low (175 $\Omega\ \mu m^2$ in the P state), making the sample able to carry large current densities without burning out. The TMR ratio was 37% at room temperature, which was defined as $(R_{AP}-R_P)/R_P$. A TMR loop over a broad field range is shown in the top left inset of Fig. 1. Measurements made at a higher field (not shown here) indicate that the pinning field was ~600 Oe. By probing the free layer, the MTJ ring shows discrete reversal steps in more detail, indicating that the sample has five magnetization states from AP to P and from P to AP, as shown in Fig. 1. These are labeled AP, M1, M2, M3, and P on the positive to negative field sweep with additional states, M4 and M5, which are present on the negative to positive field sweep. From this it can be seen that the *R-H* loop is asymmetric; an additional asymmetry is the offset in the applied field of approximately 15 Oe, which we attribute to a magnetostatic coupling to the pinned layer stack. The sign of the offset suggests that this coupling is primarily due to the orange-peel mechanism, which favors the P state. The relatively low coercivity of the free layer is consistent with its microscale size.[14]

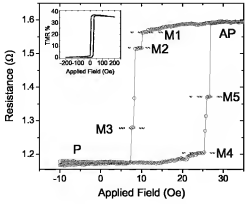

FIG. 1. (Color online) The *R-H* characteristics of the *R*-MTJ. The main figure shows in detail the metastable states achieved (M1, M2, and M3) as the junction switches from AP to P states and the M4 and M5 states that are reached while switching from P to AP. The metastable states have dashed lines to make them easier to identify. These loops are repeatable. The top left inset shows a broader field sweep with a TMR ratio of 37%.

These *R-H* measurements average over the micromagnetic state of the whole ring. Hence, to study these metastable states, micromagnetic simulations were performed on the free layer ring structure using the OOMMF code.[15] The parameters used for the simulations were as follows: saturation magnetization, $M=8\times10^5$ A m^{-1}; exchange stiffness, $A=2.8\times10^{-11}$ J m^{-1}; and the anisotropy energy constant K was set to zero so as to reflect the amorphous nature of the CoFeB. A Gilbert damping parameter $\alpha=0.5$ was used as we were not attempting to reproduce the dynamics and we desired a fast convergence. The values for M and A are based on those given by Bilzer *et al.*,[16] and while the CoFeB composition is slightly different, they suffice for simulations to qualitatively compare to the experiment. A 100×100 nm^2 cell size was used in the ring plane, while the cell depth was set to the free layer thickness. The results of converging from a uniform magnetization along the $+x$ axis at a field of +15 Oe and then sweeping the field between ±15 Oe are shown in Fig. 2. The overall simulated hysteresis loop is shown in Fig. 2(a), and the domain states at selected points marked as S1, S2, and S3 are shown in Figs. 2(b), 2(c), and 2(d), respectively. If we assume that the reference CoFeB layer in the real junction is uniformly pinned in the negative x direction, then the junction resistance gives the average moment in the free layer resolved along the x axis, since the magnetization of the free layer is known to affect the TMR via $G=\bar{G}(1+\frac{\mathrm{TMR}}{2}\cos\theta)$,[17] where G is the conductance and θ is the angle between the magnetization directions of the free and pinned layers. This means that the loops in both Figs. 1 and 2 effectively show the projection of the free layer magnetization onto the field direction.

Both measured and simulated loops contain some similar features, although they do not quantitatively match. This is not surprising, as our model discretizes a curved object onto a square mesh, which leads to unrealistic demagnetizing fields in cells at the edge (note that this can never be avoided, no matter how fine the mesh is), and also uses an ideal ring so that lithographic defects and other forms of disorder are

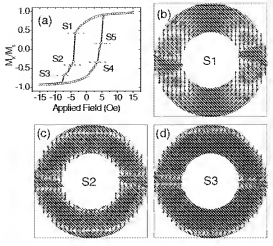

FIG. 2. (Color online) OOMMF simulations of the free layer magnetization switching of the ring MTJ. Three different metastable states can be seen in panels (b), (c), and (d) which contribute to the overall hysteresis loop shown in panel (a). Metastable states between abrupt switching events are marked as S1, S2, and S3 on the reverse-going branch and as S4 and S5 on the forward-going branch. The red-white-blue color scale in panels (b), (c), and (d) corresponds to the local x component of M (red, +ve and, blue, −ve).

not treated. Let us compare the loops: by first considering the reverse-going sweep on reducing the field to remanence, there is a smooth relaxation to a reduced net magnetization state, which continues into the reverse field regime before an abrupt jump takes place (M1 or S1 state). This relaxation is greater in the model, and we can see from Fig. 2(b) that an onion state[18] forms during this process. The greater pinning in the lithographically imperfect real sample can explain the smaller relaxation in the measured data. The magnetization then switches during a short sequence of abrupt steps via metastable states (labeled M2 and M3 or S2 and S3) to an almost fully reverse magnetized state. The S2 and S3 states are depicted in Figs. 2(c) and 2(d), respectively. The reverse-going sweep looks similar, relaxing to the M4 and S4 states, then switching to the AP state via a metastable M5 state. The fact that the magnetization does not quite saturate in the model is significant, as it is the only possible source of the asymmetry in the number of metastable states in the loop in this case. Hence, there must be some small magnetic structure remaining at the maximum field we apply which can affect the subsequent reversal of the structure, which is of the type that is known to affect the switching of rectangular magnetic elements.[19] Hence, the agreement in number between the forward and reverse switchings and the measured data is somewhat fortuitous. The absence of any pinned layer in the model means that there can be no orange-peel coupling, and the modeled loop does indeed show no overall shift.

The data plotted in Fig. 3 show that in these microscale junctions, CIMS can occur when the switching is performed starting from these metastable states for rather low current densities. By taking the data shown in Fig. 3(a) as an example, where the sample was prepared in the M4 state (an onion state) by sweeping the field from reverse saturation

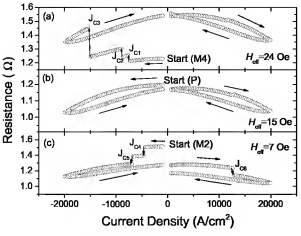

FIG. 3. (Color online) Selected $R(J)$ sweeps at different applied magnetic fields. (a) For this sweep, the applied field was set to 24 Oe, which is the position of the M4 state in Fig. 1. The M4 state is an onionlike state close to the P state. It can be seen that for an increasing applied negative current density the junction switches in three stages to an AP-like state. (b) This sweep is performed at 15 Oe, starting from the P state, at which point it can be seen from Fig. 1 that no metastable state exists and that the R-MTJ is in the P state; subsequently, there is no switching in the R-I loop. (c) The R-I loop taken at the M2 state in Fig. 1; it can be seen that the application of current causes the junction to revert to a full P state.

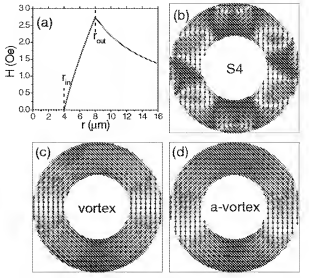

FIG. 4. (Color online) (a) Calculation of the magnitude of the Oersted field throughout the ring structure and beyond for an applied current of 11 mA. (b) The initial onionlike state of the magnetization, which corresponds to a field (3.1 Oe) just before the S4 state is reached on the forward-going branch of the loop in Fig. 2. (c) The vortex state obtained during the flow of an 11 mA current through the structure at this field. (d) The final asymmetric vortex (a-vortex) state obtained after the current was switched off. The net magnetization direction has changed from the negative to the positive x direction.

to +24 Oe, we can see that the application of a negative current led to a series of abrupt upward jumps in resistance at $J_{c1}=-7.56$ kA cm^{-2}, $J_{c2}=-9.03$ kA cm^{-2}, and $J_{c3}=-15.12$ kA cm^{-2}. On returning the current to zero, after reaching a maximum of -20 kA cm^{-2}, we found that the junction resistance was 1.54 Ω, which was very close to the resistance of the M1 state, i.e., the AP-like onion state. A subsequent application of a positive current of up to +20 kA cm^{-2} led to no further changes. The jumps were superimposed on a roughly parabolic downward trend in resistance with current bias, as would be expected for a tunneling junction due to both the nonlinear I-V and heating effects—the gradual hysteresis observed in the current sweeps arose from this second effect. Hence, while the application and removal of current to the sample can lead to changes in its magnetic state, which are inferred from the changes in resistance, the appearance of this current-driven hysteresis loop is rather different from that of the field-driven one, as shown in Fig. 1.

The M4 state had a resistance of 1.20 Ω, which was only 0.03 Ω higher than the P state. The highest field at which the P state was observed was +15 Oe on the forward-going sweep (Fig. 1), and the same current cycling was performed at this value of field: The results are displayed in Fig. 3(b). It can be seen that no CIMS was observed. This means that J_C needed for the full switch from the AP to the P state was greater than ~20 kA cm^{-2}. Hence, an important result of this work is that the presence of the onion state is required for this form of low current density CIMS.

It was also possible to drive the junction to switch in the opposite manner, as shown in Fig. 3(c): Starting from the M2 state (1.52 Ω), the current was swept in the same way as was previously done for a fixed field of +7 Oe. Two downward jumps in resistance were observed at $J_{c4}=-5.00$ kA cm^{-2} and $J_{c5}=-6.91$ kA cm^{-2}. At zero current, the device resistance was 1.27 Ω, which was almost exactly the same value at the M3 state. A further application of positive currents led to another downward jump at $J_{c6}=+7.94$ kA cm^{-2}, with the final device resistance being that of the P state, i.e., 1.17 Ω. It is worth noting that in both cases present in Figs. 3(a) and 3(c), most of the switching occurred for negative currents; nevertheless, they represent switching in opposite directions. This is inconsistent with the usual effects of spin-transfer torque in CIMS, where a change in the sense of the switching current leads to a change in the sense of the switching.

In general, the current can influence the magnetization of the free layer either through the Slonczewski spin-transfer torque[4] or the Oersted field. Given that spin-transfer effects are inconsistent with our data, it seems likely that the explanation is the Oersted field H_i, which for such a ring structure is given by

$$H_i = \frac{I}{2\pi r}\left(\frac{r^2 - r_{in}^2}{r_{out}^2 - r_{in}^2}\right), \tag{1}$$

where I, r, r_{in}, and r_{out} are the applied current, the distance from the center of the ring, the inner radius, and the outer radius of the ring, respectively. This was calculated for a typical applied current (11 mA) throughout the ring structure, and the results are shown in Fig. 4(a). The peak value of H_i is around 2.5 Oe, which is similar to the fields giving rise to the steps of the metastable states in Figs. 1 and 2. Thus, this

could explain the CIMS observed, although, of course, the Oersted field is of a right-hand screw form. Our calculation here was performed using a uniform current distribution, which will be valid when the MTJ is in either the AP or P state, but only an approximation for the intermediate states, where current crowding in locally P regions will lead to slightly larger local peak fields.

To see if this Oersted field could be the cause of the CIMS we observed, we further performed some simple micromagnetic calculations by taking into account both the Oersted field effects and a Slonczewski-like spin-transfer torque term arising from a uniform current density in the z direction, i.e., normal to the layers. We selected a point on the forward-going branch of the field-driven hysteresis loop [Fig. 2(a)] just before the S4 state is reached, where $H=3.1$ Oe. The micromagnetic structure of the ring at this point is shown in Fig. 4(b), which is a complex state with mainly onionlike character with $M_z/M_{sat}=-0.18$. With the field held at this value, a current of 11 mA (corresponding to a current density of 7.29 kA cm^{-2}) was applied to the structure in the z direction. The spin polarization of the current was set to zero so that no spin-transfer effects would take place. The resulting Oersted field leads to an almost perfect vortex state, as depicted in Fig. 4(c); this state has $M_x/M_{sat}=0$. After the current is switched off, this state relaxes into an asymmetric vortex state, as shown in Fig. 4(d), with $M_x/M_{sat}=+0.09$: The magnetization partly relaxes into the direction of H. Indistinguishable effects resulted from the same calculation with the spin polarization of both layers set to 0.45, which is a reasonable value for CoFeB,[20] and the fixed layer polarization directed along the pinning direction, showing that spin-transfer effects play no role at these low current densities.

In summary, we observed five metastable magnetization states in the field-driven hysteresis loop of a microscale ring-shaped MTJ. When magnetization was prepared in one of these states, a current-driven switching was observed at a very low current density, which was only about 10^4 A cm^{-2}, with the switching in both directions activated by currents of the same sign. Switching was not observed when the starting point was a well-defined P state. A micromagnetic modeling of the ring-shaped free layer qualitatively reproduces the metastable states, and also indicates the mechanism by which the low current density CIMS is achieved: the Oersted field generated by the current produces a vortex state, lifting the system out of its local energy minimum associated with the metastable state. When the current is switched off, it can then relax into the applied field direction. This explains the marked difference in the overall form of the R-H and R-I free layer loops. Similar metastable states have also been observed in 100 nm diameter MTJs, where spin torque dominates the CIMS.[21]

The authors would like to thank A. T. Hindmarch for fruitful discussions and M. Donahue for sharing a prerelease version (1.2a4) of the OOMMF code with us. In China, this work was supported by the State Key Project of Fundamental Research of Ministry of Science and Technology Grant No. 2006CB6932200, by the Knowledge Innovation Program project, and by the Wong Kuancheng Project of the Chinese Academy of Sciences. X.-F.H. is grateful for the partial support of the Outstanding Young Researcher Foundation (Grants No. 50325104 and No. 50528101) and to the National Natural Science Foundation of China (Grant No. 10574156). In the United Kingdom, this work was supported by the EPSRC, partly through the Spin@RT consortium.

*xfhan@aphy.iphy.ac.cn
†c.h.marrows@leeds.ac.uk

[1] W. J. Gallagher and S. S. P. Parkin, IBM J. Res. Dev. **50**, 5 (2006).
[2] J.-G. Zhu, Y. Zheng, and G. Prinz, J. Appl. Phys. **87**, 6668 (2000).
[3] L. Berger, Phys. Rev. B **54**, 9353 (1996).
[4] J. C. Slonczewski, J. Magn. Magn. Mater. **159**, L1 (1996).
[5] F. J. Albert, J. A. Katine, R. A. Buhrman, and D. C. Ralph, Appl. Phys. Lett. **77**, 3809 (2000).
[6] A. A. Tulapurkar, Y. Suzuki, A. Fukushima, H. Kubota, H. Maehara, K. Tsunekawa, D. D. Djayaprawira, N. Watanabe, and S. Yuasa, Nature (London) **438**, 339 (2005).
[7] G. D. Fuchs, N. C. Emley, I. N. Krivorotov, P. M. Braganca, E. M. Ryan, S. I. Kiselev, J. C. Sankey, D. C. Ralph, R. A. Buhrman, and J. A. Katine, Appl. Phys. Lett. **85**, 1205 (2004).
[8] J. C. Sankey, Y.-T. Cui, J. Z. Sun, J. C. Slonczewski, R. A. Buhrman, and D. C. Ralph, Nat. Phys. **4**, 67 (2008).
[9] H. Kubota, A. Fukushima, K. Yakushiji, T. Nagahama, S. Yuasa, K. Ando, H. Maehara, Y. Nagamine, K. Tsunekawa, D. D. Djayaprawira N. Watanabe, and Y. Suzuki, Nat. Phys. **4**, 37 (2008).
[10] Z. Diao, D. Apalkov, M. Pakala, Y. Ding, A. Panchula, and Y. Huai, Appl. Phys. Lett. **87**, 232502 (2005).
[11] Y. Liu, Z. Zhang, P. P. Freitas, and J. L. Martins, Appl. Phys. Lett. **82**, 2871 (2003).
[12] X. F. Han, S. F. Zhao, and A. C. C. Yu, Sci. Technol. Adv. Mater. **6**, 784 (2005).
[13] S. F. Zhao, J. Zhao, Z. M. Zeng, X. F. Han, A. C. C. Yu, Y. Ando, and T. Miyazaki, IEEE Trans. Magn. **41**, 2636 (2005).
[14] H. X. Wei, T. X. Wang, Z. M. Zeng, X. Q. Zhang, J. Zhao, and X. F. Han, J. Magn. Magn. Mater. **303**, e208 (2006).
[15] M. J. Donahue and D. G. Porter, National Institute of Standards and Technology, Technical Report No. NISTIR 6376, 1999; Version 1.2a4 of the software was used, which can treat Oersted fields and Slonczewski-type spin-transfer torques arising from uniform current densities (http://math.nist.gov/oommf).
[16] C. Bilzer, T. Devolder, J.-V. Kim, G. Counil, C. Chappert, S. Cardoso, and P. P. Freitas, J. Appl. Phys. **100**, 053903 (2006).
[17] J. C. Slonczewski, Phys. Rev. B **39**, 6995 (1989).
[18] J. Rothman, M. Kläui, L. Lopez-Diaz, C. A. F. Vaz, A. Bleloch, J. A. C. Bland, Z. Cui, and R. Speaks, Phys. Rev. Lett. **86**, 1098 (2001).
[19] K. J. Kirk, J. N. Chapman, and C. D. W. Wilkinson, Appl. Phys. Lett. **71**, 539 (1997).
[20] D. X. Wang, C. Nordman, J. M. Daughton, Z. H. Qian, and J. Fink, IEEE Trans. Magn. **40**, 2269 (2004).
[21] Z. C. Wen, H. X. Wei, and X. F. Han, Appl. Phys. Lett. **91**, 122511 (2007).